Conformation and Electron-transfer Chemistry in Model Photosynthetic Reaction Centres Determined by Fast Atom Bombardment Mass Spectrometry†

Stephen Naylor,*,‡,[a] James A. Cowan,§,[b] John H. Lamb,[a] Christopher A. Hunter[b] and Jeremy K. M. Sanders*,[b]

[a] *MRC Toxicology Unit, Carshalton, Surrey SM5 4EF, UK*

[b] *Cambridge Centre for Molecular Recognition, University Chemical Laboratory, University of Cambridge, Lensfield Road, Cambridge CB2 1EW, UK*

Fragment ions, derived from a series of capped and dimeric porphyrins subjected to fast atom bombardment mass spectrometry (FAB-MS), provide supporting evidence for the production of porphyrin excited states generated during the FAB process. Such excited states lead to intramolecular electron-transfer reactions, that can be investigated using FAB-MS. The excited state model is further developed when applied to two multicomponent porphyrins. Consideration of fragmentation and metal ion uptake by such compounds in FAB-MS allowed confirmation of the geometry of these porphyrins and also provided an understanding of the multiple intramolecular electron-transfer processes occurring. It is demonstrated that stringent geometry and symmetry requirements are needed for such molecules to function as special pair electron-donors in charge separation reactions.

Naturally occurring porphyrins play an important role in numerous biological, biochemical and geochemical processes.[1] However, there is a growing interest in complex synthetic porphyrins, such as strapped,[2] capped[3] and 'picket fence'[4] systems, in order to investigate host–guest complexation,[5] modelling of the photosynthetic reaction centre,[6] catalysis in artificial enzyme mimics[7] and their use in photodynamic therapy.[8]

Mass spectral analysis of low molecular weight monomeric porphyrin derivatives has been readily achieved using electron ionization (EI)[9] and chemical ionization (CI)[10] mass spectrometry, as well as CI tandem mass spectrometry.[11] However, cofacial dimeric and strapped porphyrins are not particularly amenable to analysis using such techniques because of their increased molecular weight and lability. The analysis of such molecules required the development of soft ionization desorption methods such as field desorption (FD),[12] laser desorption (LD)[13] and fast atom bombardment (FAB)[14] mass spectrometry. FD-MS has been useful in providing molecular weight information on a series of porphyrins,[9c,d] but most success has been found in the analysis of porphyrins through the use of either LD[15] or FAB-MS.[16] (Although Aplin[9d] has reported some success with 'In beam' EI.) In previous work we have described the behaviour of monomeric and dimeric metalloporphyrins in a number of different matrices in FAB-MS and noted a striking similarity with the solution chemistry of such molecules;[16c] in particular with their photoinduced electron-transfer chemistry.

In this paper we describe the dominant factors determining the fragmentation of dimeric porphyrins, plus the uptake of added metal ions by free-base porphyrins in the FAB matrix. The behaviour of a series of capped and dimeric porphyrins provides supporting evidence for the model of the complex series of reactions that occur in the FAB matrix we described previously.[16c] Our observations on these dimeric and strapped porphyrins are used to investigate the preferred conformations of the two multi-component molecules **$H_4$1** and **$H_4$2**. We

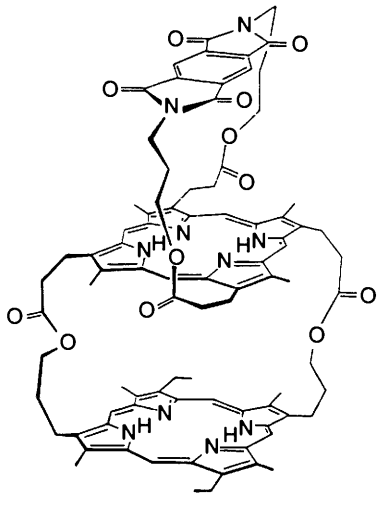

$H_4$1

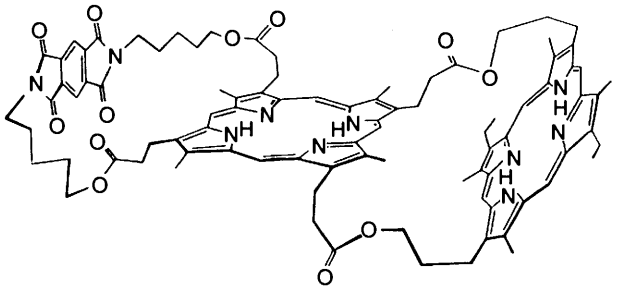

$H_4$2

† A preliminary account of this work was presented as a poster at the Second International Symposium on Applied Mass Spectrometry. Barcelona, 1990.

‡ *Present address:* Grainger Mass Spectrometry Facility, Mayo Clinic, Rochester. MN 55905. USA.

§ *Present address:* Evans Laboratory of Chemistry. Ohio State University. Columbus. Ohio 43210. USA.

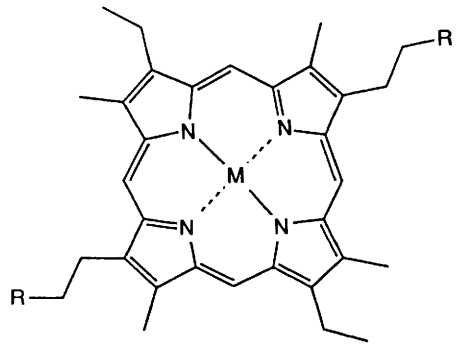

	M	R
3	2H	CH_2OH
	2H	CO_2Me
4	or Cu(II), Co(II) Co(III), Mn(III)	CO_2Me

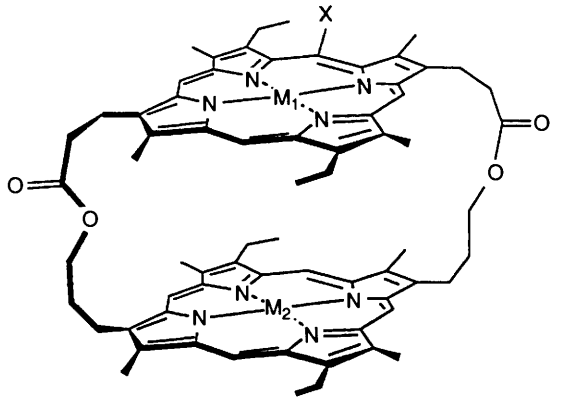

5

X	M_1	M_2
H	2H	2H
H	2H	Zn(II)
H	Co(III)	2H
H	Mn(III)	2H

6

NO_2	2H	2H
NO_2	2H	Zn(II)

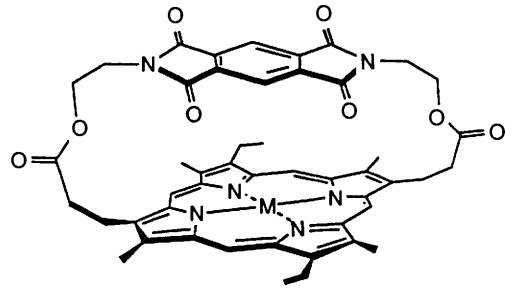

7

demonstrate how FAB-MS may be used to investigate the multiple intramolecular electron-transfer processes that make these complex porphyrins good candidates for artificial photosynthetic systems. Moreover, our results have important implications for understanding and modelling the behaviour of the bacterial photosynthetic reaction centre. We demonstrate that there are strong geometry and symmetry requirements for a porphyrin dimer to function as a 'special pair' electron-donor in charge separation reactions.[1b,6a]

Results and Discussion

Fragmentation of Porphyrins in FAB-MS.—The fragment ion abundance observed in FAB-MS is typically 1–10% of the molecular ion signal.[14b,17] Although the overall fragment ion yield is low, useful structural information can often be obtained from consideration of such fragment ions. We investigated the behaviour of monomeric, dimeric and bridged porphyrins in positive and negative ion FAB-MS and looked at the common fragment ions obtained under bombardment conditions with a view to establishing the conformations and properties of the two closely related complex porphyrins, H_4**1** and H_4**2**.

(a) *Monomeric porphyrins.* A series of free base [*meso*-II-porphyrin diol (H_2**3**) and *meso*-II-porphyrin dimethylester (DME) (H_2**4**)] and metalloporphyrins (such as Cu^{II}**4**, Co^{II}**4**, Mn^{III}**4** and Co^{III}**4**) were subjected to both positive and negative ion FAB-MS. In all cases, fragment ions were observed that corresponded to loss of the peripheral methyl and alkyl substituent side chains. There was no marked evidence of breakdown of the central aromatic porphyrin macrocycle. This contrasts with the results obtained in CI-MS,[10,11] and LD-MS[15c] in which substantial fragmentation of the pyrrole ring system occurs.

In positive ion FAB-MS both H_2**3** and H_2**4** afforded identical fragment ion clusters in the mass range 380–500 daltons corresponding to multiple-bond cleavages.* These ion clusters are centred 14 mass units apart and are ~ 1–3% of the molecular

* In all cases single bond cleavages corresponding to loss of methyl (−15), ethyl (−29) and –C(O)OMe (−59) were also observed.

ion abundance. In the case of $Mn^{III}4$ the fragment ion cluster centres are shifted by +52 Da, to 440–550 Da (as shown in Fig. 1), corresponding to a gain of Mn^+ with concomitant loss of 3 hydrogens. This indicates the presence of the intact tetrapyrrole ring system, with fragmentation only occurring at the side chains. Fragment ion abundance from $Mn^{III}4$ varies from *ca.* 3–5% of the molecular ion abundance. The observed increase in fragment ion abundance of $Mn^{III}4$ compared to H_23 and H_44 presumably reflects the presence of the preformed ion Mn^+ in the intact tetrapyrrole ring fragment ions.

The fragment ion clusters, separated by 14 Da, consist of *ca.* 6–8 ions and are presumably attributable to the fragment ion (F) series $[F^{\bullet+}$, $(F - xH)^{\bullet+}$ and $F + xH)^{\bullet+}]$ and $[FH^+$, $(FH - xH)^+$ and $(FH + xH)^+]$. Possible fragment ion structures for FH^+ are shown in Fig. 2 for H_24 and $Mn^{III}4$. Obviously these ions could also arise from an unsymmetrical cleavage of the sidechains.

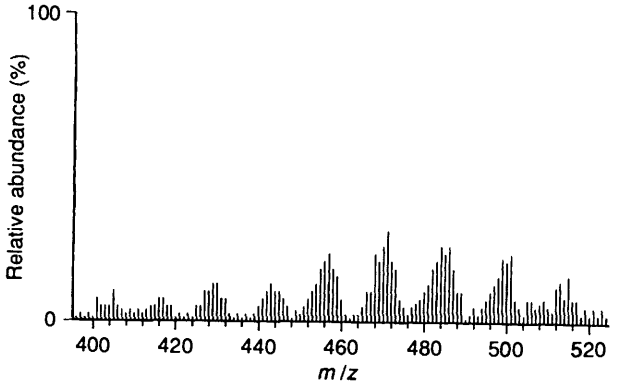

Fig. 1 Positive ion FAB-MS, after background subtraction of matrix ions (NBA), of $Mn^{III}4$ for the mass range 395–525 Da

The negative ion FAB-MS of H_24 contains the familiar ion clusters, 14 mass units apart, but shifted by +44 Da from the positive ion clusters. This reflects retention of a carboxylate group (CO_2^-) on one of the sidechains.

(b) *Capped porphyrins and cofacial dimers.* In these dimeric systems, the basic tetrapyrrole and aromatic nucleii remain intact so the fragmentation is dominated by cleavage of the ester side chain straps. The fragmentation patterns observed in both positive and negative ion FAB-MS are summarized in Table 1. These results may be rationalized on the basis of four competing mechanisms which determine the charges associated with the two faces of the dimers.

1. *Remote-site fragmentation.* Remote-site fragmentation [18] of the ester side chain straps should result in the diacid face of the porphyrin being detected in negative ion FAB-MS whereas the diol face should be observed in the positive ion mode.

2. *Pre-formed charge.* Porphyrins which contain trivalent metals such as $Mn^{III}H_25$ and $Co^{III}H_25$ are positively charged and so derived fragment ions should appear in the positive ion FAB-MS.

3. *Redox properties of the porphyrin.* The better electron-accepting porphyrin face will be observed in negative ion FAB-MS, whereas the better electron-donating face will predominate in positive ion FAB-MS.

4. *Intramolecular electron-transfer.* In electron donor–acceptor compounds such as H_27, the generation of excited states in the selvedge zone can lead to intramolecular electron-transfer.[16c] If this process is very efficient, the electron-donor face should be observed as a positive fragment ion while the electron-acceptor should be observed as a negative fragment ion.

At first sight, mechanisms 3 and 4 appear to be identical, but

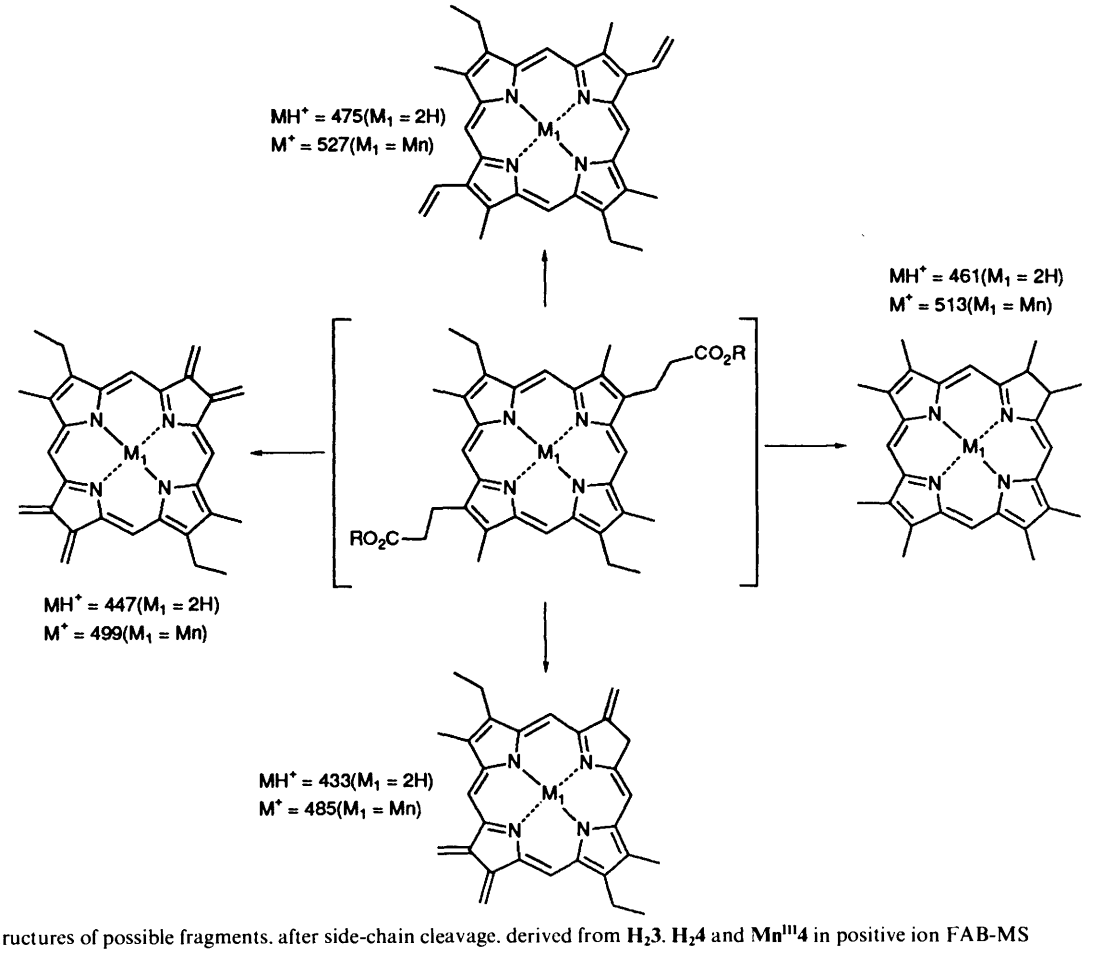

Fig. 2 Structures of possible fragments, after side-chain cleavage, derived from H_23, H_24 and $Mn^{III}4$ in positive ion FAB-MS

Table 1 Summary of fragment ions observed in both positive and negative ion FAB-MS for a number of capped and strapped porphyrin molecules

Compound	+ve or −ve FAB-MS	Directing mechanism of fragmentation: Pre-formed ion	Remote site fragments	Redox properties	Fragments observed in FAB-MS
$H_4$5	+ve	N/A[a]	Diol[b]	N/P[d]	~380–480[e]
	−ve	N/A	Diacid[c]	N/P	Diacid
$Mn^{III}H_2$5	+ve	Diacid	Diol	Diacid	Diacid
	−ve	N/A	Diacid	Diol	Diacid
$H_4$6	+ve	N/A	Diol	Diol	Diol
	−ve	N/A	Diacid	Diacid	Diacid
$Zn^{II}H_2$6	+ve	N/A	Diol	Diol	Diol
	−ve	N/A	Diacid	Diacid	Diacid
$H_2$7	+ve	N/A	Py[f]	Diacid	~3:1 Diacid:Py
	−ve	N/A	Diacid	Py	~3:1 Py:Diacid

[a] N/A not applicable. [b,c] Refers to the porphyrin face containing either the diol or diacid functionality. [d] N/P not predictable. [e] Refers to the mass range where fragment ions were observed. [f] Py: pyromellitimide functionality.

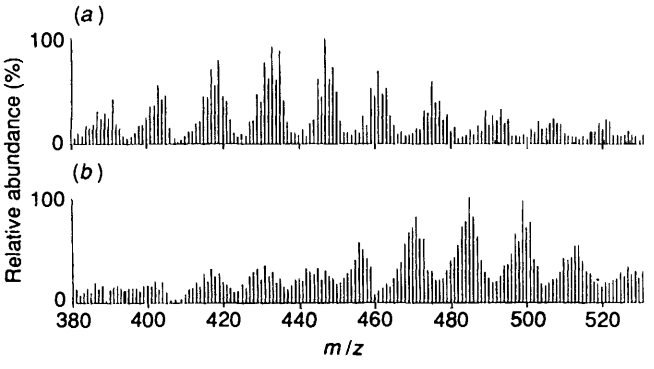

Fig. 3 Positive ion FAB-MS, after background subtraction of matrix ions (NBA), of fragment ion region 380–530 Da for (*a*) **$H_4$5**; (*b*) **$Mn^{III}H_2$5**

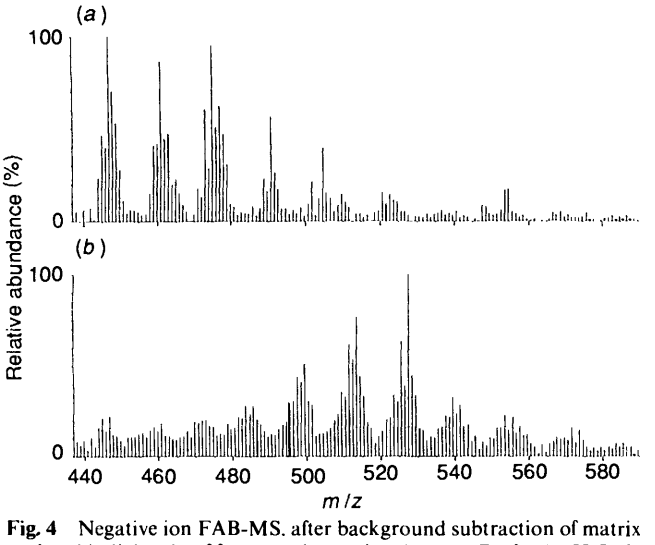

Fig. 4 Negative ion FAB-MS, after background subtraction of matrix peaks (thiodiglycol), of fragment ion region 440–550 Da for (*a*) **$H_4$5**; (*b*) **$Mn^{III}H_2$5**

there is a fundamental difference. If mechanism 3 dominates, then the fragment ions observed for the adducts will show similar distributions to the mass spectra obtained for the individual monomers. However, if mechanism 4 dominates, then the fragment ion patterns will differ from those observed for the individual monomers. Studies of the photophysical properties of donor–acceptor systems such as **$H_2$7** show that the properties of the adducts amount to more than the sum of the properties of the individual components: the adducts perform intramolecular photoinduced electron-transfer. Thus, if the mass spectra of the donor–acceptor adducts differ from the sum of the spectra of the individual monomers as in mechanism 4, FAB-MS must be sensitive to the new supramolecular properties of the adducts. In other words, FAB-MS could be used to probe the electron-transfer properties of such assemblies.

The positive ion FAB mass spectrum of the symmetrical cofacial porphyrin dimer (CFD) (**$H_2$5**) exhibited fragment ion clusters in the mass range ~380–490 Da, as shown in Fig. 3(*a*). These ions arise from a double remote site cleavage of the straps, followed by further loss of sidechain functional groups as previously described for compounds **$H_2$3** and **$H_2$4**. Perusal of the negative ion FAB-MS of **$H_4$5**, as shown in Fig. 4(*a*) reveals that the fragment ion clusters are shifted by + ~44 Da into the mass range ~430–530 Da, reflecting the dominance of remote site fragmentation to afford fragment ions containing the $-CO_2^-$ functional groups.

The positive ion FAB-MS of NO_2–CFD (**$H_4$6**) displays fragment ions between ~380–490 Da (*cf.* **$H_4$5**) attributable to the unsubstituted porphyrin face, but no fragment ions are observed for the nitro-containing porphyrin face (45 mass units higher than the unsubstituted porphyrin fragment ion clusters). Similarly, with $Zn^{II}NO_2$–CFD (**$Zn^{II}H_2$6**) (in which the metal is in the diol face), there were no detectable fragment ions corresponding to the nitro-containing porphyrin face, whereas porphyrin fragment ion clusters appeared between ~440–560 Da indicating the presence of Zn in the porphyrin diol face. The negative ion FAB-MS of NO_2–CFD (**$H_4$6**) and $Zn^{II}NO_2$–CFD (**$Zn^{II}H_2$6**) both revealed fragment ion clusters in the mass range ~470–560 Da corresponding to the nitro-containing face complete with the presence of the CO_2^- group. These results can all be rationalized on the basis of the remote-site fragmentation mechanism. Similarly, the **$Zn^{II}H_2$5** results are consistent with this remote-site fragmentation mechanism (Table 1).

Examination of the positive ion FAB-MS of **$Mn^{III}H_2$5**, shown in Fig. 3(*b*), reveals fragment ion clusters in the mass range ~440–530 Da indicating the presence of Mn in the tetrapyrrole ring system. Since the metal is located in the acid face of the dimer, if remote site fragmentation was the dominant factor then the diol face with fragment ion clusters in the mass range ~380–490 Da should be observed. However, in this instance, the presence of the pre-formed positive charge associated with the trivalent metal directs the fragmentation clusters observed. A similar result is obtained for **$Co^{III}H_2$5** (results not shown) except that the ion clusters are shifted by +4 mass units reflecting the change $^{55}Mn \longrightarrow {}^{59}Co$. The corresponding negative ion FAB-MS of **$Mn^{III}H_2$5** [Fig. 4(*b*)] shows ion clusters derived from the diacid face containing Mn, reflecting the dominance of remote-site fragmentation in determining the negative fragment ion abundance (reduction of $Mn^{III} \longrightarrow Mn^{II}$ can neutralize the preformed charge, as described previously [16c]).

Consideration of BPC-2 (**$H_2$7**) leads to the prediction that if

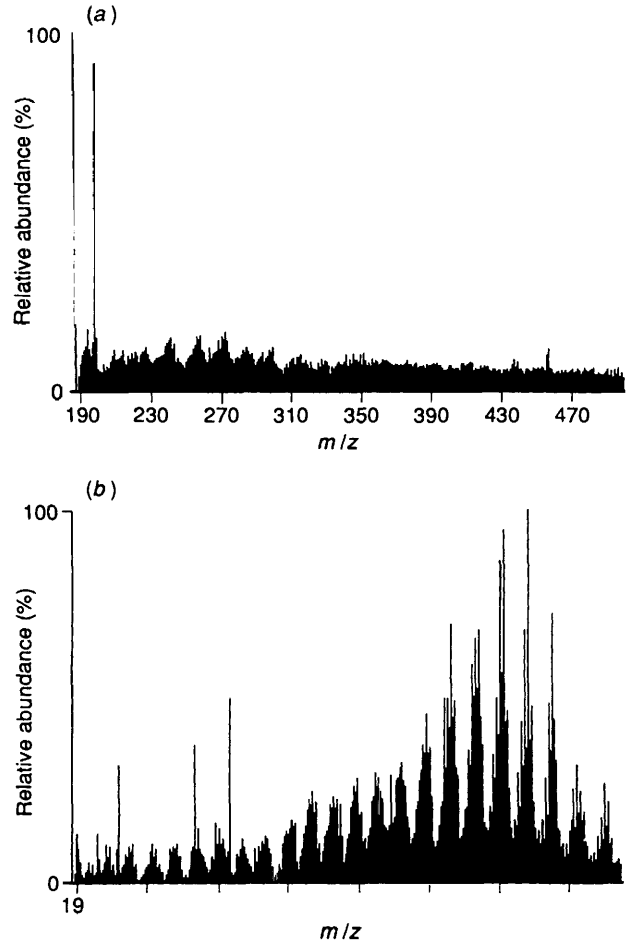

Fig. 5 (*a*) Negative ion FAB-MS, after background subtraction of matrix peaks (NBA). of fragment ion region 190–500 Da for BPC-2 (**H_27**); (*b*) Positive ion FAB-MS, after background subtraction of matrix peaks (thioglycerol–glycerol, 1:1) of fragment ion region 190–500 Da

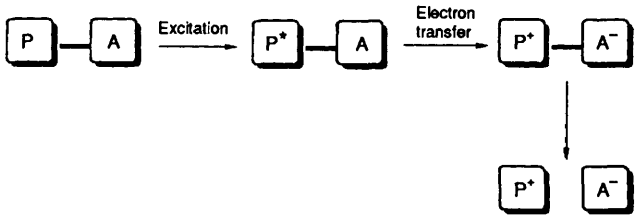

Fig. 6 Excited state model of electron-transfer reactions occurring in capped and dimeric porphyrins in FAB-MS

remote-site fragmentation dominates, then pyromellitimide clusters should be observed in positive ion FAB-MS, and fragment ions assignable to the porphyrin face should be observed in the negative ion mode. The experimental results [see Fig. 5(*a*)] show that pyromellitimide fragment cluster ions (~220–280 Da) dominate the negative ion FAB-MS of **H_27**. In the positive ion FAB-MS [Fig. 5(*b*)] the porphyrin face fragment ion clusters (~380–500 Da) are most abundant. There are also positive fragment ions assignable to the pyromellitimide face (~220–280 Da), but these ions are only *ca.* 25–30% of the ion abundance of the porphyrin species. All these observations are in accord with the redox properties of the molecule determining types of fragment ions formed.

It is interesting to note that when the individual components that make up these dimeric systems are examined separately (*e.g.* **H_23**, **H_24**, **NO_2–H_24**, and bisalkyl pyromellitimide) abundant molecular ions are observed in both negative and positive ion FAB-MS. Thus, our results indicate that by linking two aromatic groups in a cofacial arrangement we have modified their properties with respect to FAB ionization.

All these observations are consistent with the model that we have recently developed (summarized in Fig. 6) *to explain* the behaviour of porphyrins in FAB-MS.[16c] Bombardment of the matrix containing porphyrin induces an excited state, followed by intramolecular electron transfer. This generates a pyromellitimide radical anion and porphyrin radical cation. Subsequent fragmentation of the ester side chain straps allows these products to dissociate and since both radicals are relatively stable species, they should have reasonably long lifetimes in the selvedge region. Hence, pyromellitimide fragment ions dominate the negative FAB-MS spectrum while porphyrin fragments are most abundant in the positive ion spectrum. This result demonstrates that mechanism 4 can determine fragmentation patterns and suggests that FAB-MS may be a useful tool for investigating electron-transfer in supramolecular assemblies.

Uptake of Metal Ions by Free Base Porphyrins.—Addition of an aqueous solution of $Zn(OAc)_2$ to the FAB matrix containing the cofacial dimer CFD (**H_45**) results in the appearance of two additional ions in the positive ion FAB spectrum at m/z = 1131 and 1193, corresponding to $[(H_45 + {}^{64}Zn - 2H) + H]^+$ and $[(H_45 + 2{}^{64}Zn - 4H) + H]^+$, respectively. After 3 min in the fast atom (xenon) beam, the ratio CFD:ZnCFD:Zn_2CFD was 3:2.5:1. Clearly a substantial number of the free base porphyrins are metallated by zinc ions either in the matrix or the selvedge zone. If a monometallated CFD such as Mn^{III}CFD (**$Mn^{III}H_25$**) is subjected to the same conditions, an ion at m/z = 1183 corresponding to ^{64}ZnMnCFD (**$Mn^{III}Zn^{II}5$**) is observed. The ratio MnCFD:ZnMnCFD is 3:2 after 1 min and continues to decrease until the ZnMnCFD ion abundance is greater than the MnCFD parent ion after 5 min. This series of experiments demonstrates that if a free base porphyrin is available then uptake of an available metal ion such as Zn^{2+} is rapid. Similar results were obtained with the simple monomeric porphyrins, **H_23** and **H_24**.

Mass Spectral Analysis of Complex Porphyrins.—The two multicomponent systems, **H_41** and **H_42**, were each synthesised as a pair of diastereoisomers.[6a] Such complex assemblies of chromophores have the potential to mimic the behaviour of the photosynthetic reaction centre,[1,6] but factors which affect electron-transfer processes in such systems are still poorly understood.[19] We demonstrate here that FAB-MS is a useful tool for investigating both the conformation and the electron-transfer properties of such assemblies.

The fragmentation of **H_42** is conceptually similar to that of BPC-2 (**H_27**). The positive ion FAB-MS gave a molecular ion. MH^+, at m/z = 1509 plus fragment ions in the range 1000–1080 Da and 400–500 Da (Table 2). The 1000–1080 Da fragments correspond to porphyrin dimers, *i.e.* simple loss of the pyromellitimide cap. The 400–500 Da fragments are again monomeric porphyrin units corresponding to loss of the pyromellitimide and a porphyrin face. The negative ion FAB-MS showed only fragment ions in the 300–400 Da region. corresponding to the pyromellitimide group. Thus electron-transfer reactions lead to the formation of a porphyrin radical cation (or a porphyrin dimer radical cation) and a pyromellitimide radical anion.

Addition of a small amount of either $Zn(OAc)_2$ or $Mn(OAc)_2$ (results not shown) to the matrix (either NBA or thiodiglycol) containing **H_42** resulted in uptake of the metal cation in accord with our results for the simple cofacial dimers. Ions corresponding to the uptake of both one and two metals were observed almost immediately upon addition of the metal ions to

Table 2 Ratio of molecular ion abundance for **$H_4$1** and **$H_4$2**, and their bismetallated, and monometallated molecular ions, plus the ratio of molecular ion abundance and fragment ions in the region 1000–1150 Da and 400–500 Da. All ratios were determined in positive ion FAB-MS using thiodiglycol as matrix after the samples had been in the fast atom beam for 1 min

	Metallated molecular ion ratios		Fragment ion ratios	
	MH^+	MH^+	MH^{+a}	MH^{+a}
	$(2ZnH)^+$	$(ZnH)^+$	1000–1150	400–550
$H_4$1	—	—	12:1	N/D[b]
$ZnH_2$1	N/D	3:1	11.5:1	9:1
$H_4$2	—	—	12:1	8:1
$ZnH_2$2	1.2:1	1:1	7:1	8:1

[a] Fragment ion abundance determined by measuring the most abundant ion cluster in the mass range under consideration. [b] N/D: not detected above background, even after 5 min in fast atom beam.

the matrix. After 3 min in the xenon beam no MH^+ at m/z = 1509 was observed, and the ratio **$ZnH_2$2**:**$Zn_2$2** was 1:1. The fragment ions observed for the metallated species, **$ZnH_2$2** and **$Zn_2$2**, were similar to those from the parent free base compounds but were shifted by $\sim +60$ Da indicating the incorporation of Zn (Table 2). We observed fragment ions in the regions 1060–1200 Da (dimers) and 440–560 Da (monomers).

The positive ion FAB-MS of **$H_4$1** was remarkably different from that of **$H_4$2** (Table 2). We observed an abundant molecular ion MH^+ at m/z = 1453, but no low mass fragment ions in the mass range 400–500 Da were detected. The only major fragment ions were in the range 1000–1080 Da, attributable to porphyrin dimers, corresponding to simple loss of the pyromellitimide group. Again the negative ion FAB-MS showed only fragment ions corresponding to the pyromellitimide group in the region 240–360 Da.

Addition of $Zn(OAc)_2$ or $Mn(OAc)_2$ (results not shown) to the matrix containing **$H_4$1** again resulted in uptake of the metal cation. However, we observed a molecular ion corresponding to uptake of only one metal (either Mn or Zn). The bismetallated species was not detected, even after 10 min in the fast atom beam. In addition, the fragment ions observed for the metallated derivative, **$ZnH_2$1**, were surprisingly different from those from the parent freebase compound (Table 2). **$ZnH_2$1** exhibited fragment ions in the region 440–560 Da, corresponding to a zinc porphyrin monomer. There were no fragment ions due to monomeric free base porphyrins which would be observed at *ca.* 60 mass units lower. The abundance of fragment ions in the range 1000–1080 Da, due to the porphyrin dimers which dominated the **$H_4$1** fragmentation pattern, was significantly reduced (Table 2).

We rationalize the behaviour of these two complex porphyrin adducts on the basis of their stereochemistry and photophysical properties. Spectroscopic studies show that **$H_4$1** and **$H_4$2** adopt substantially different conformations in solution.[6a] In **$H_4$1**, the three chromophores are confined to a cofacial 'stacked' arrangement as evidenced by exciton coupling of the porphyrin electronic transitions in the UV spectrum (*cf.* cofacial dimers) and large upfield shifts of the pyromellitimide and porphyrin *meso*-proton signals in the ^1H NMR spectrum.[20] The spectra of **$H_4$2** lack these features, indicating that it prefers a more 'open' geometry (see structures). Our metallation studies provide further evidence for these conformational preferences. **$H_4$1** can only be metallated once, showing that the central porphyrin in the 'sandwich' is sterically shielded. The outside porphyrin and pyromellitimide π-stack with the central porphyrin[5e] and block the second metal binding site. The geometry of **$H_4$2** is radically different: it adopts an 'open' conformation so that metallation of both porphyrins is easy. As with the simple dimeric systems, the fragmentation patterns provide evidence of the electron-transfer processes occurring in these assemblies. Our results not only correlate well with detailed studies of the electron-transfer reactions in **$H_4$1** and **$H_4$2** (using time-resolved picosecond fluorescence spectroscopy),[6a] they also throw light on the requirements for 'special pair' behaviour.[16a,19] With **$H_4$2**, we observed both monomeric and dimeric porphyrin fragment ions in the positive ion FAB-MS, but, with **$H_4$1**, only dimers were observed. As with BPC-2 (**$H_4$7**), excitation of the porphyrin leads to an electron-transfer reaction with the formation of a pyromellitimide radical anion and porphyrin radical cation. However, with **$H_4$1**, the radical cation is delocalized over both porphyrins. This is a very stable species so that fragmentation to yield porphyrin monomers is highly unfavourable. The chromophore arrangement in **$H_4$2** does not permit such delocalization and so further fragmentation of the dimer occurs. Photophysical measurements have shown that subsequent to photoinduced electron-transfer in these systems, **$H_4$1** forms a more stable charge-separated state than **$H_4$2**. This was attributed to the fact that in **$H_4$1** the two porphyrins can act in concert as a single delocalized unit in the same way as the 'special pair' in the photosynthetic reaction centre.[6a]

Our results may have important implications for understanding and modelling the behaviour of the photosynthetic reaction centre.[5e,6,19] The primary electron donor in the bacterial photosynthetic reaction centre is a 'special pair' bacteriochlorophyll dimer.[1] The two chromophores are held in a cofacial arrangement and interact strongly.[19] However, the significance of the geometry of the 'special pair' interchromophore interaction is only beginning to be understood.[5e,6a,19] Our results clearly demonstrate that if two porphyrins are held in a cofacial arrangement, as in **$H_4$1**, electron-transfer reactions lead to the formation of very stable radical cations. For other geometries (*e.g.* **$H_4$2**) such a dramatic stabilization of the radical is not possible. Electrochemical measurements on cofacial porphyrin dimers have shown that the formation of a radical cation is stabilized by *ca.* 0.1 eV relative to the corresponding monomer in solution.[21] The fragmentation we observe probably occurs in the gas phase where such effects are likely to be enhanced.[5e]

In the light of this discussion, the fragmentation patterns observed with the metallated derivatives are very illuminating. The behaviour of the two derivatives is again straightforward since there is no inter-chromophore interaction. However, with **$Zn^{II}H_2$1**, the 'special pair' behaviour is disrupted by metallation. Monomer fragments are now observed and the dimer signal is very weak, *i.e.* the **$Zn^{II}H_2$1** dimer fragments are relatively unstable. Moreover, only metallated porphyrin monomer cations are observed. We can rationalize this behaviour on the basis of the porphyrin redox potentials. Zinc porphyrins are good electron-donors and in solution a zinc porphyrin monomer radical cation is more stable than a porphyrin dimer radical cation by *ca.* 0.1 eV. Thus electron transfer in **$Zn^{II}H_2$1** probably proceeds *via* a two-step sequential process (Fig. 7). Excitation leads to electron transfer from the free base porphyrin (the primary donor) to the pyromellitimide (the acceptor). However, a delocalized porphyrin dimer radical cation is not favourable in this system and a second electron transfer from the zinc porphyrin to the free base porphyrin occurs. Thus the major fragment ions are a pyromellitimide radical anion and a monomeric zinc porphyrin radical cation, and it appears that symmetry is an essential prerequisite for 'special pair' behaviour.

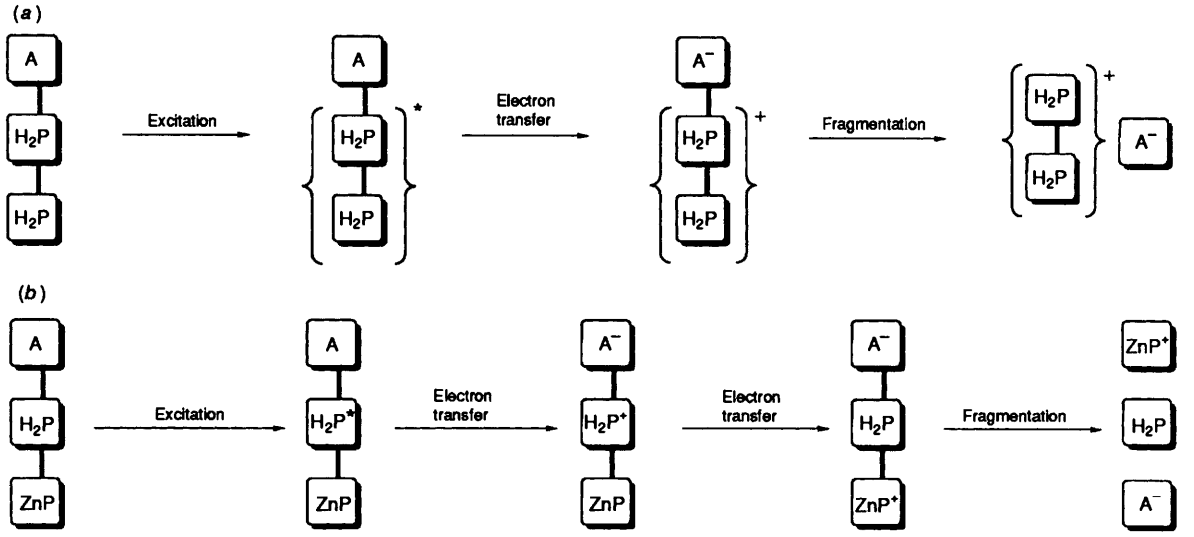

Fig. 7 Electron-transfer processes occurring in: (*a*) H_4**I**; (*b*) **Zn**H_2**I** as determined by FAB-MS

Conclusions

We have presented a model which explains the fragment patterns of complex bridged and dimeric porphyrins in FAB-MS. The striking feature of these patterns is that when electron donor–acceptor systems are studied, relatively abundant fragment ions corresponding to the electron-donor are observed in positive ion FAB-MS, while fragment ion clusters corresponding to the electron-acceptor are observed in negative ion FAB-MS. This contrasts with the behaviour of the individual donor and acceptor components when they are studied separately; both can be observed in positive and negative ion FAB. This implies that FAB-MS is sensitive to intramolecular reactivity, in this case electron-transfer between the donor and the acceptor. Previously, we have shown that porphyrin excited states are generated in FAB-MS and that these excited states lead to intramolecular electron-transfer reactions that are very similar to photoinduced electron transfer reactions.[16c] The observations in this paper show that by examining the fragment ions in both positive and negative ion FAB-MS, it is possible to examine the products of such electron-transfer reactions in multichromophore assemblies.

This work opens an exciting range of new applications for FAB-MS in the study of electron-transfer reactions and, in particular, in the study of complex porphyrin assemblies that mimic the behaviour of the photosynthetic reaction centre. We have illustrated the potential of this technique with some experiments on complex porphyrins that reproduce the charge separation reactions of the primary events in photosynthesis.[1,6] The ability of free base porphyrins to take up free metal ions in the FAB matrix was first used to ascertain the geometry of the two complex porphyrins and these geometries were then correlated with electron-transfer reactions in these systems, as deduced from the FAB-MS fragmentation patterns. Our investigations have elucidated some requirements for 'special pair' behaviour in porphyrin dimers and help in developing a model for the function and behaviour of the different components which make up the bacterial photosynthetic reaction centre.[1,6,19] A symmetrical cofacial arrangement is essential for a porphyrin dimer to function as a 'special pair'. Such 'special pair' behaviour manifests itself in the formation of a highly stabilized radical cation dimer subsequent to electron transfer. Metallation of one of the porphyrins disrupts this behaviour and leads to a two step sequential electron-transfer reaction.

Experimental

Materials and Samples.—All solvents used were HPLC grade. The FAB-MS matrices glycerol, thioglycerol, aminoglycerol, thiodiglycol, tetraglyme and 3-nitrobenzylalcohol were all purchased from Aldrich Chemical Co., UK and were vacuum distilled prior to use. Zinc acetate and manganese acetate were purchased from Aldrich and used without further purification.

The synthesis and purification of all porphyrins used in this work have been described previously.[6a,20,22]

Mass Spectra.—All FAB mass spectra were recorded on either a Kratos MS-50 or a VG 70-SEQ mass spectrometer, as described in our previous work.[16c]

Acknowledgements

We thank the MRC (S. N., J. H. L.), SERC (J. A. C., J. K. M. S) and Dept. of Education, Northern Ireland (C. A. H.) for financial support.

References

1 See, *e.g.*, (*a*) A. R. Fersht, *Enzyme Structure and Mechanism*, W. H. Freeman, Reading, 1985; (*b*) J. Diesenhofer and H. Michel, *Angew. Chem., Int. Ed. Engl.*, 1989, **28**, 829; (*c*) G. Eglington, in: *Mass Spectrometry in the Health and Life Sciences*, eds. A. L. Burlingame and N. Castagnoli, Jr., Elsevier, Amsterdam, p. 47, 1985.
2 J. P. Collman, C. S. Bencosme, R. R. Durand, R. P. Kreh and F. C. Anson, *Org. Mass Spectrom.*, 1983, **105**, 2699.
3 J. E. Almog, J. E. Baldwin, R. L. Dyer and M. Peters, *J. Am. Chem. Soc.*, 1975, **97**, 226.
4 J. P. Collman, R. R. Gagne, C. A. Reed, T. R. Halvert, G. Lang and W. T. Robinson, *J. Am. Chem. Soc.*, 1975, **97**, 1427.
5 (*a*) A. D. Hamilton, J.-M. Lehn and J. L. Sessler, *J. Am. Chem. Soc.*, 1986, **108**, 5158; (*b*) H. L. Anderson and J. K. M. Sanders, *Angew. Chem., Int. Ed. Engl.*, 1990, **30**, 1440; (*c*) C. A. Hunter, M. N. Meah and J. K. M. Sanders, *J. Am. Chem. Soc.*, 1990, **112**, 5773; (*d*) H. L. Anderson, C. A. Hunter, M. N. Meah and J. K. M. Sanders, *J. Am. Chem. Soc.*, 1990, **112**, 5781; (*e*) C. A. Hunter and J. K. M. Sanders, *J. Am. Chem. Soc.*, 1990, **112**, 5525.
6 (*a*) J. A. Cowan, J. K. M. Sanders, G. S. Beddard and R. J. Harrison, *J. Chem. Soc., Chem. Commun.*, 1987, 55; (*b*) J. L. Sessler, M. R. Johnson and T.-Y. Lin, *Tetrahedron*, 1989, **45**, 4767; (*c*) D. Gust and T. A. Moore, *Science*, 1989, **244**, 35; (*d*) M. Wasielewski, M. P. Niemczyk, W. A. Svec and E. B. Pewitt, in: *Antennas and Reaction Centers of Photosynthetic Bacteria*, ed. M. E. Michael-Beyerle, Springer-Verlag, Berlin, p. 242, 1985.

7 (*a*) J. T. Groves and R. Neumann. *J. Am. Chem. Soc.*, 1989. **111**, 2900; (*b*) R. P. Bonar-Law and J. K. M. Sanders. *J. Chem. Soc., Chem. Commun.*. 1991. 574.
8 (*a*) *Porphyrins in tumour phototherapy*. eds. A. Andreoni and R. Cubeddu. Plenum. New York, 1984; (*b*) *Photodynamic therapy of tumours and other diseases*. eds. G. Jori and C. Perria, Librena Progretto. Padova, 1985.
9 (*a*) K. M. Smith. in: *Porphyrins and Metalloporphyrins*, ed. K. M. Smith. Elsevier, Amsterdam, p. 381, 1975; (*b*) A. H. Jackson. *Phil. Trans. Royal Soc. London. A*. 1979. **293**, 21; (*c*) Budzikiewicz. in: *The Porphyrins*. ed. D. Dolphin, Wiley, New York. p. 395, vol. III, 1982; (*d*) R. T. Aplin, in *Mass Spectrometry in the Health and Life Sciences*. eds. A. L. Burlingame and N. Castagnoli Jr.. Elsevier, Amsterdam, 1985. p. 171.
10 (*a*) B.-R. Tolf. X.-Y. Jiang, A. Wegmann-Szente, L. A. Kehres, E. Bunnenberg and C. Djerassi, *J. Am. Chem. Soc.*, 1986, **108**, 1363; (*b*) G. J. Van Berkel. G. L. Glish, S. A. McLuckey and A. A. Tuinman, *J. Am. Chem. Soc.*. 1989. **111**. 6027.
11 G. J. Van Berkel. G. L. Glish, S. A. McLuckey and A. A. Tuinman, *Anal. Chem.*, 1990. **62**. 786.
12 H. D. Beckey, *Field Ionization Mass Spectrometry*, Pergamon Press, Oxford, 1979.
13 See. *e.g.*. (*a*) C. F. Ijames and C. L. Wilkins, *J. Am. Chem. Soc.*, 1988, **110**. 2687; (*b*) L. M. Nuwaysir and C. L. Wilkins, *Anal. Chem.*, 1988, **60**, 279.
14 (*a*) M. Barber. R. S. Bordoli, G. J. Elliot, R. D. Sedgwick and A. N. Tyler. *Anal. Chem.*. 1982, **54**, 645A; (*b*) C. Fenselau and R. J. Cotter, *Chem. Rev.*. 1987. **87**. 501.
15 (*a*) J. Grotemeyer, U. Boest, K. Walter and E. W. Schlag, *Org. Mass Spectrom.*, 1986, **21**, 645; (*b*) L. M. Nuwaysir and C. L. Wilkins, *Anal. Chem.*, 1989. **61**. 689; (*c*) T. H. Nguyen, P. S. Clezy, G. D. Willett, G. L. Paul, J. Tann and P. J. Derrick, *Org. Mass Spectrom.*, 1991, **26**, 215.
16 (*a*) B. D. Musselman, D. Kessel and C. K. Chang, *Biomed. Environ. Mass Spectrom.*, 1988, **15**, 257; (*b*) R. K. Pandey, M. M. Siegel, R. Tsao, J. H. McReynolds and T. J. Dougherty, *Biomed. Environ. Mass Spectrom.*, 1989, **18**, 405; (*c*) S. Naylor, C. A. Hunter, J. A. Cowan, J. H. Lamb and J. K. M. Sanders, *J. Am. Chem. Soc.*, 1990, **112**, 6507.
17 S. Naylor and G. Moneti, *Biomed. Environ. Mass Spectrum.*, 1989. **18**, 405.
18 See for a review. J. Adams, *Mass Spectrom. Rev.*, 1990, **9**, 141.
19 (*a*) A. Warshel and W. W. Parson, *J. Am. Chem. Soc.*, 1987, **109**, 6143 and 6152; (*b*) A. Warshel, S. Creighton and W. W. Parson, *J. Am. Chem. Soc.*, 1988, **92**. 2696; (*c*) S. F. Fischer and P. O. Scherer. *J. Chem. Phys.*, 1987. **115**, 151.
20 C. A. Hunter, J. K. M. Sanders and A. J. Stone, *Chem. Phys.*, 1989. **133**, 395.
21 J. A. Cowan and J. K. M. Sanders, *J. Chem. Soc., Perkin Trans. 1*. 1987, 2395.
22 J. A. Cowan and J. K. M. Sanders, *J. Chem. Soc., Perkin Trans. 1*, 1985, 2435.

Paper 1/04846E
Received 19*th September* 1991
Accepted 19*th November* 1991